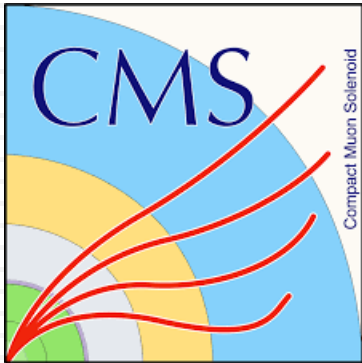


Calibration and performance of the CMS Electromagnetic Calorimeter in LHC



Jin Wang¹

1: Institute of High Energy Physics, CAS

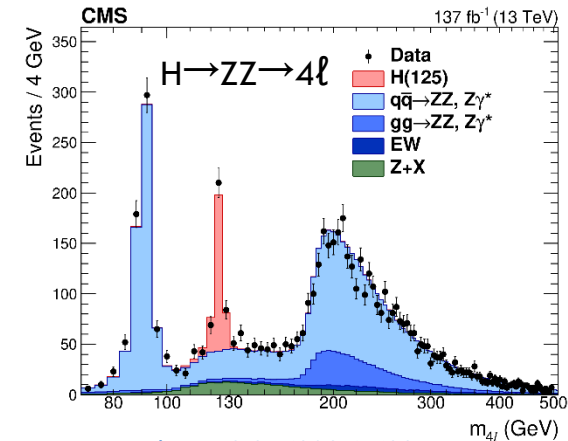
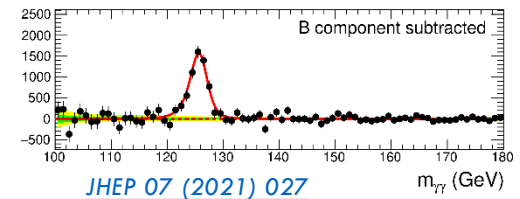
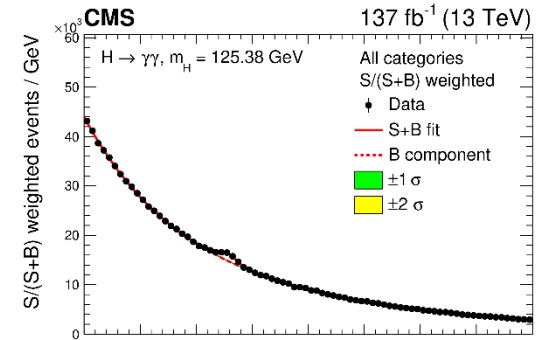
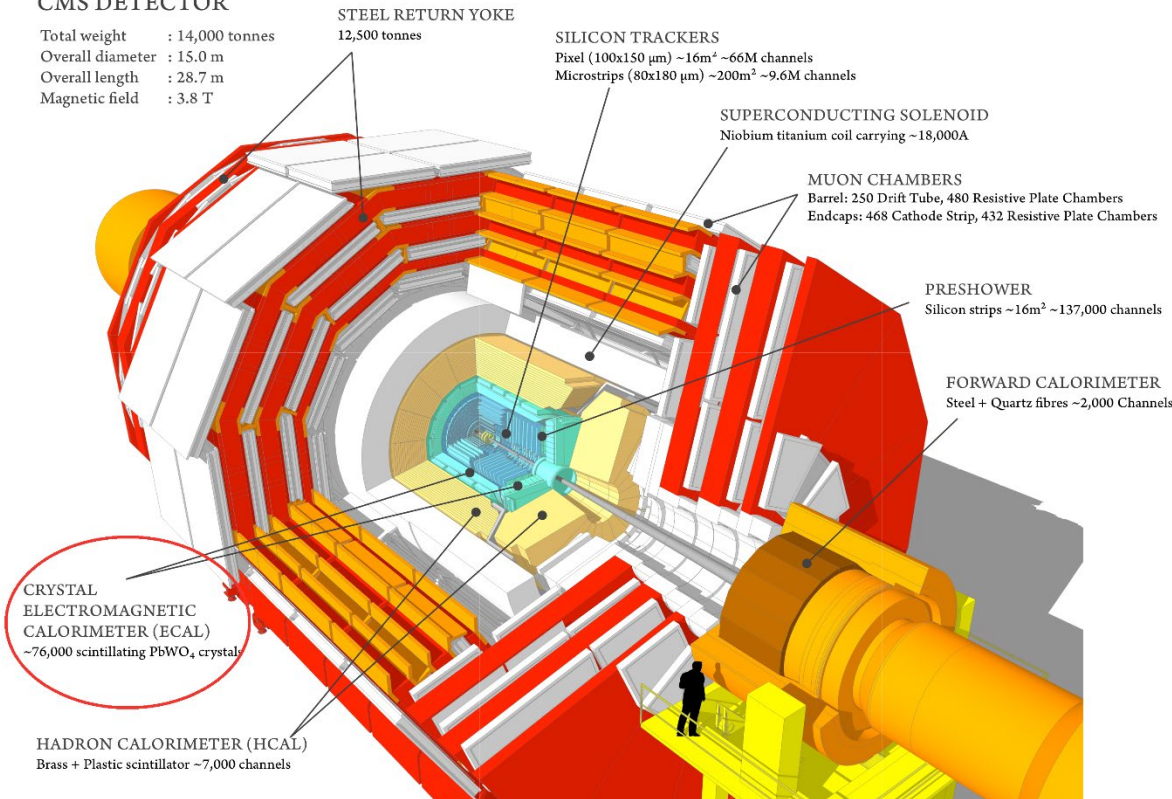
CMS Electromagnetic Calorimeter (ECAL)

2

- CMS is a general-purpose detector designed to
 - test Standard Model (SM) predictions
 - search for new physics beyond the SM

CMS DETECTOR

Total weight : 14,000 tonnes
 Overall diameter : 15.0 m
 Overall length : 28.7 m
 Magnetic field : 3.8 T



- The electromagnetic calorimeter plays a crucial role in many CMS physics analyses that involve electrons/photons/jets

CMS Electromagnetic Calorimeter (ECAL)

3

- ECAL: compact, homogeneous, hermetic and fine-grain crystal calorimeter
 - designed to provide highly efficient and accurate reconstruction of photons and electrons

- 75848 lead tungstate crystals PbWO_4
- high density of 8.3 g/cm^3
- short radiation length 0.89 cm
- small Moliere radius 2.2 cm
- fast light emission : $\sim 80\%$ in $\sim 25 \text{ ns}$



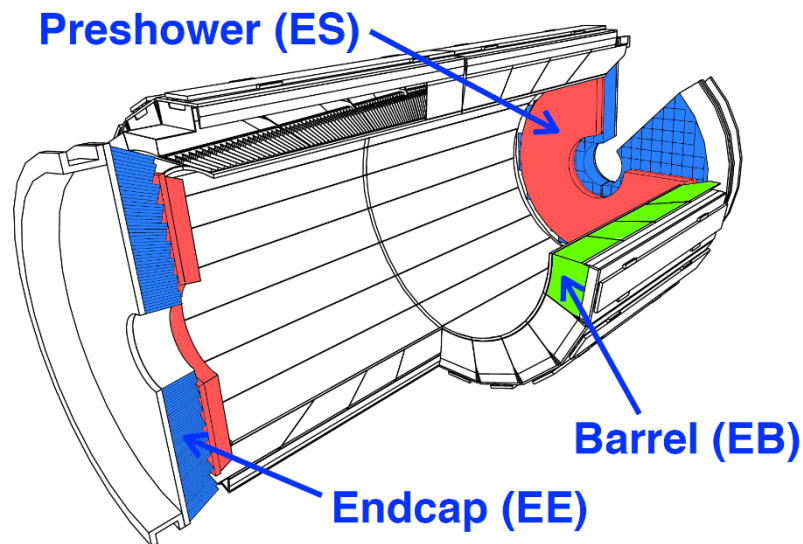
Coverage:

Barrel (EB): $|\eta| < 1.48$

Endcap (EE): $1.48 < |\eta| < 3.0$

Preshower (ES): $1.65 < |\eta| < 2.6$

(ES: discriminate between prompt photons and photons from π_0 decay)



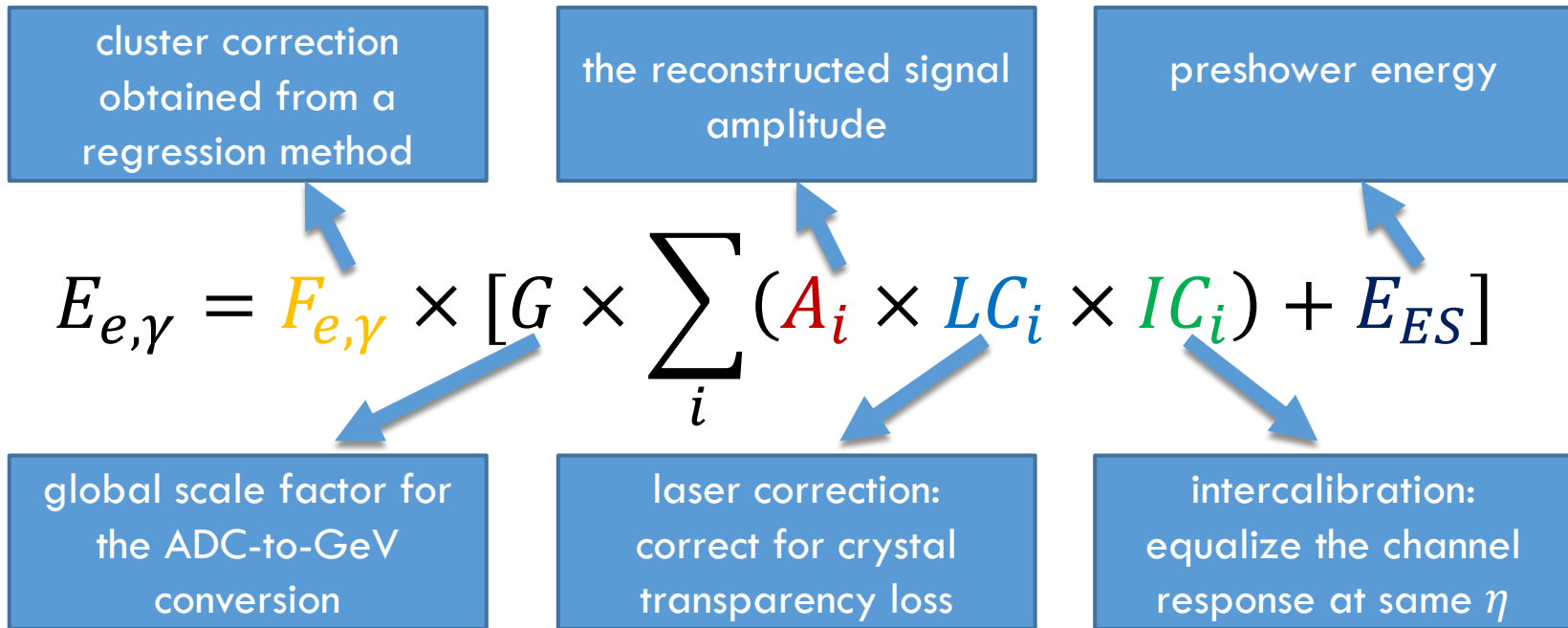
ECAL challenges in LHC Run 2:

- higher pileup and noise, increased exposure to radiation
- a larger variation of the calorimeter response that must be corrected for

ECAL signal reconstruction

4

- Electromagnetic particles deposit their energy over several ECAL crystals.
 - dynamic clustering algorithms used to collect the energy deposits in ECAL
- The reconstructed energy of electrons and photons is estimated by:

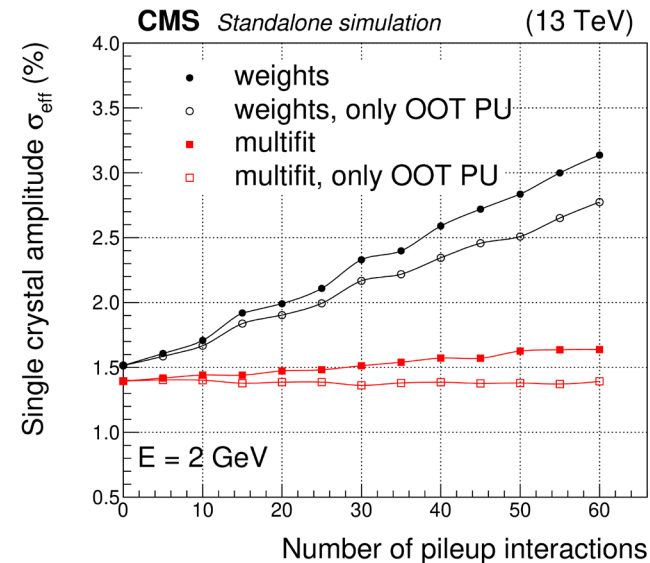
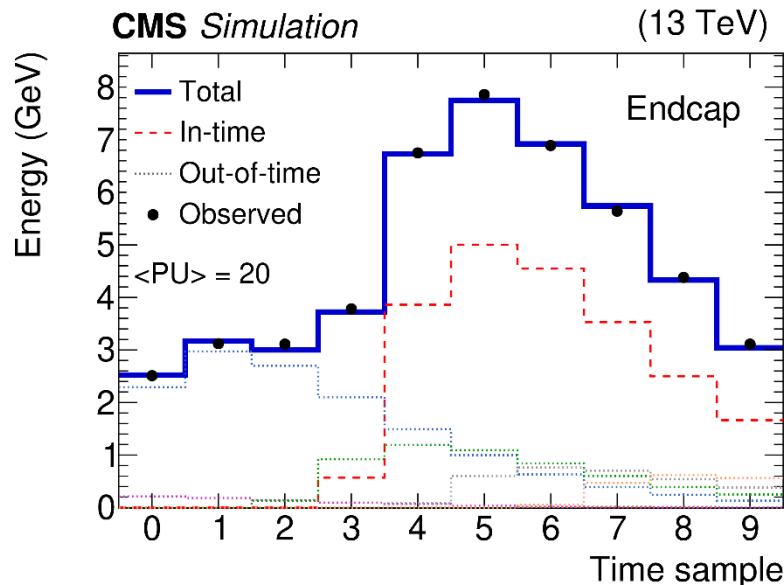


Signal amplitude reconstruction (A_i)

5

- 10 digitized ECAL pulse samples recorded for signal amplitude reconstruction
 - one in-time pulse and up to 9 out-of-time (OOT) pulses
 - Run 1: amplitude reconstructed from a weighted sum of samples
 - Run 2: 'multifit' reconstruction method used to mitigate higher pileup

[JINST 15 \(2020\) P10002](#)



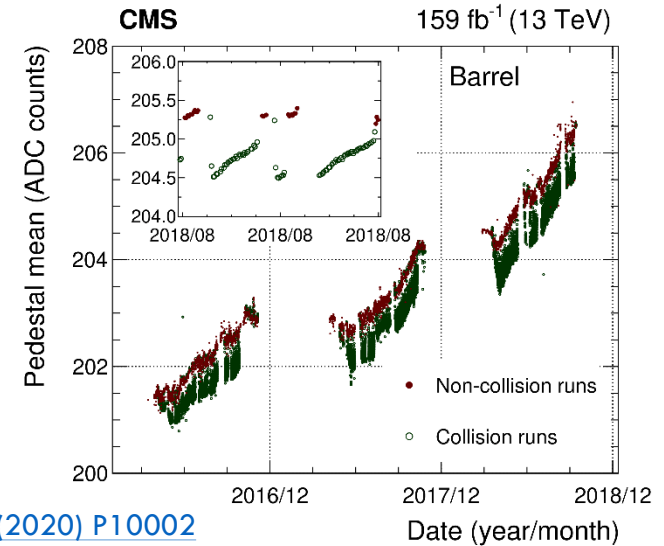
- The 'multifit' reconstruction method is robust against pile-up increase.

Pedestal condition and timing calibration

6

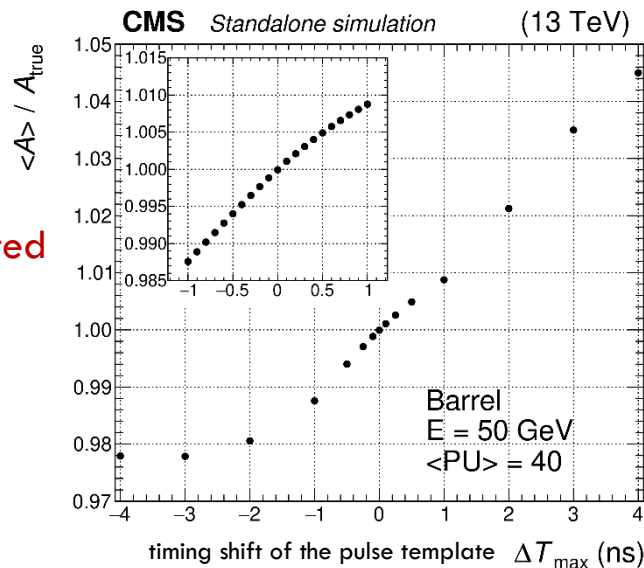
- Pedestal from high gain measured from laser events every 40 minutes.
- Pulse shapes updated weekly in Run 3
- Time shift due to irradiation corrected every week
 - towards negative times during collisions and towards positive times during recovery

Pedestal mean over time for ECAL barrel

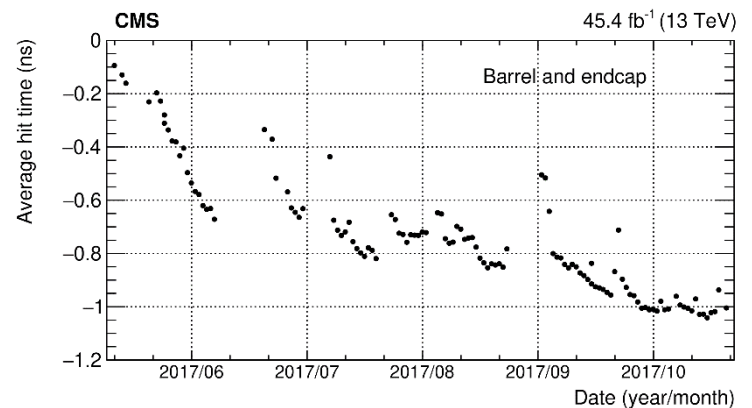


[JINST 15 \(2020\) P10002](#)

Good agreement
between reconstructed
amplitude over true
amplitude



Average ECAL pulse timing in 2017

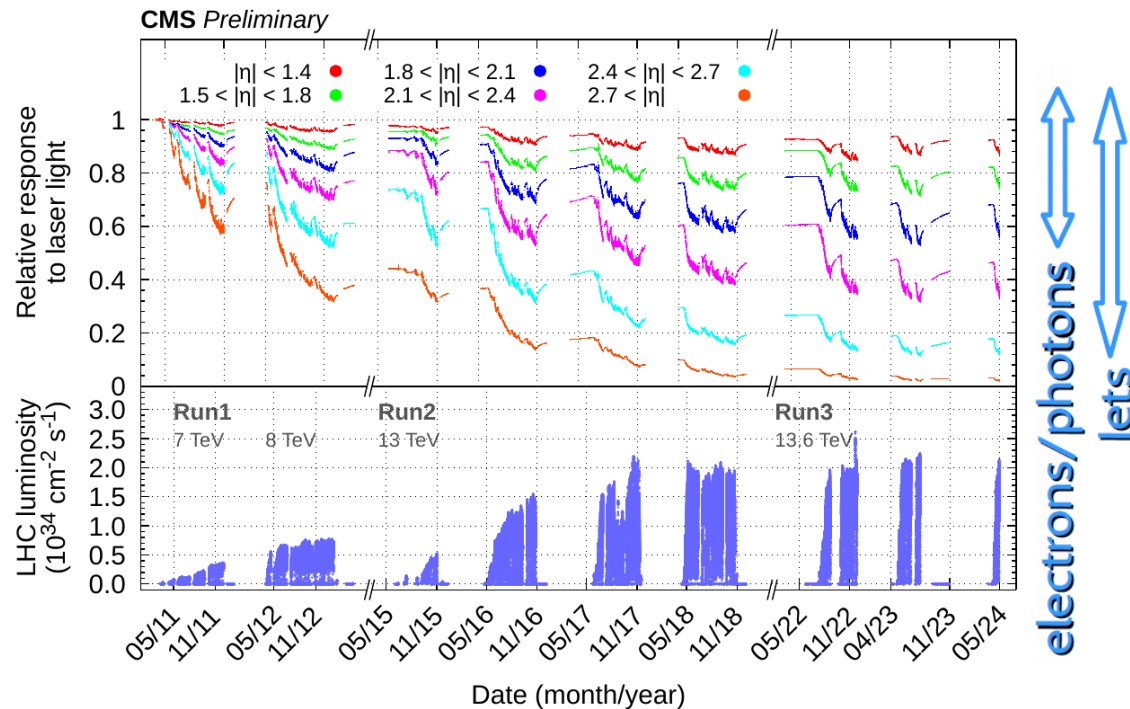


ECAL transparency loss

7

- ECAL channel response varies with time due to radiation-induced effects
 - crystal transparency changes over time
 - photocathode aging with accumulated charge

[CERN-CMS-DP-2024-022](#)



Transparency loss correction is crucial to maintain stable ECAL energy scale and resolution over time

Laser Correction (LC_i)

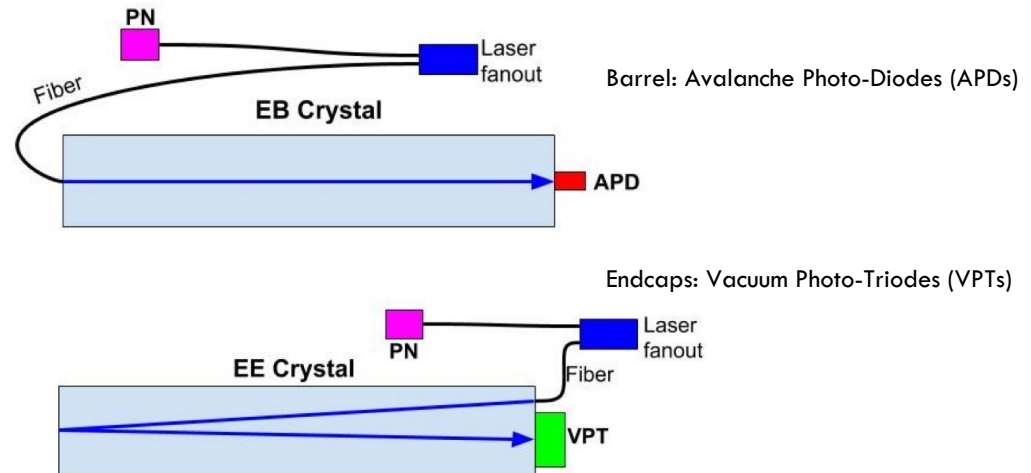
8

- A dedicated laser monitoring system is designed to provide corrections for transparency changes.
 - injects laser light with a wavelength of 447nm into each crystal
 - relates ECAL channel response variation to changes in the scintillation signal
 - measures the calibration point per crystal every 40 minutes
 - obtains and applies corrections within 48 hours for the prompt reconstruction

$$\frac{S(t)}{S_0} = \left(\frac{R(t)}{R_0} \right)^\alpha$$

Correction for e/y scintillation (pink arrow pointing to $S(t)$)
Response to injected laser (blue arrow pointing to $R(t)$)
 α parameter (red arrow pointing to α)

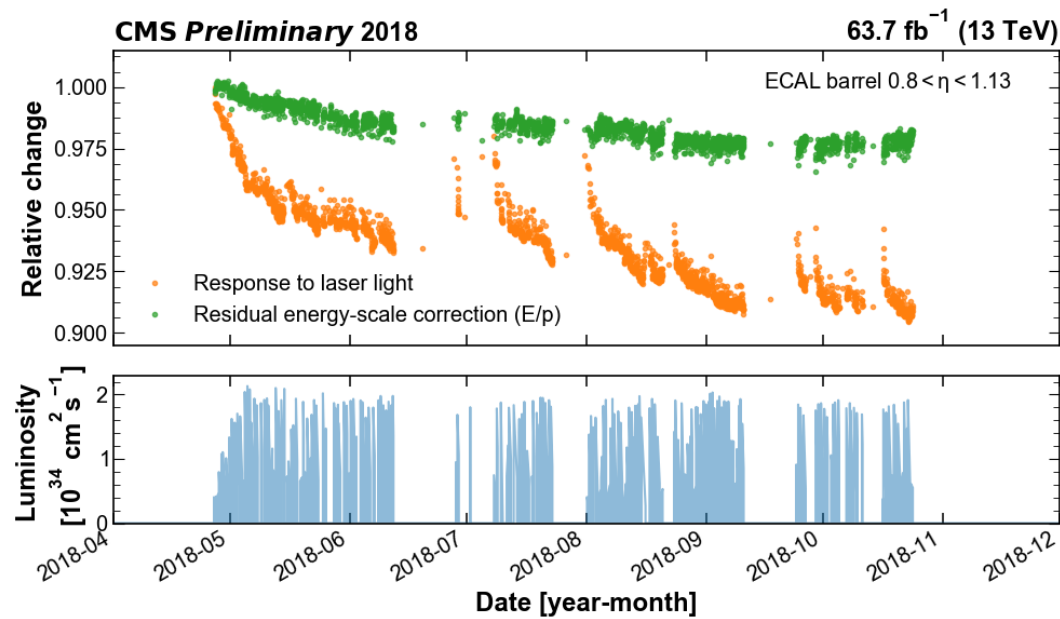
Relative response = APD(VPT) / PN



- α parameter depends on η and evolves with integrated luminosity
 - periodically re-computed to ensure energy scale stability and high resolution

Laser correction with E/p residual correction

9



[CMS-DP-2019/030](#)

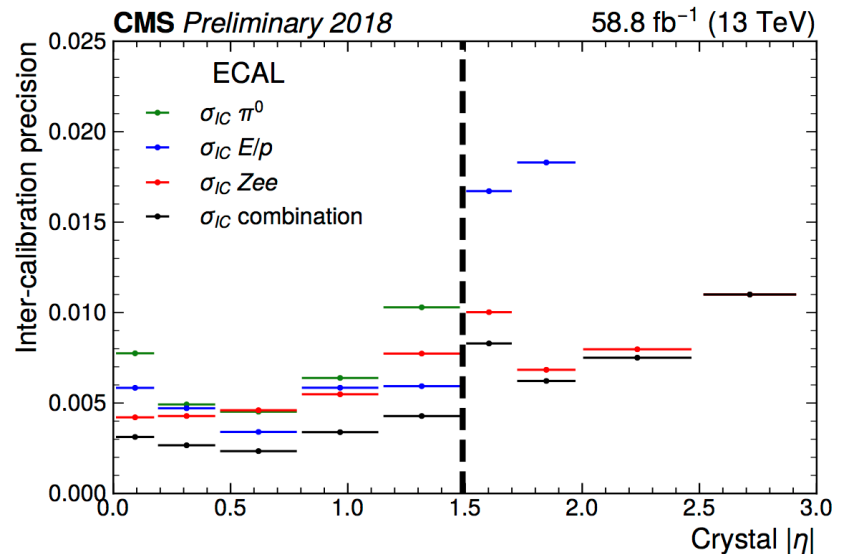
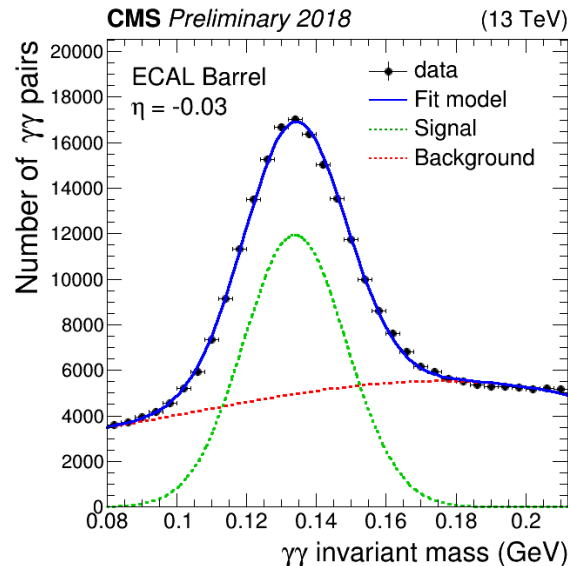
- Orange: relative response variations to laser light injected in the ECAL crystals
- Green: the residual energy-scale correction after the application of the laser corrections
 - correction needed due to a drift of the response of the PN diode used in the laser-based calibration system, determined by comparison with the tracker-measured momentum of electrons from W/Z bosons (E/p ratio)
 - a few percent variation the whole year and independent of instantaneous luminosity

Intercalibration (IC_i)

10

- IC: equalize the ECAL response for different crystals at the same η coordinate.
- A combination of several methods based on different physics signals
 - π^0 mass: exploit reconstructed π^0 mass with its decay of photon pairs
 - E/p: comparison of the ECAL energy to the tracker momentum for isolated electrons from W/Z boson decay
 - Zee: exploit the invariant mass reconstructed with electron pairs from Z decays

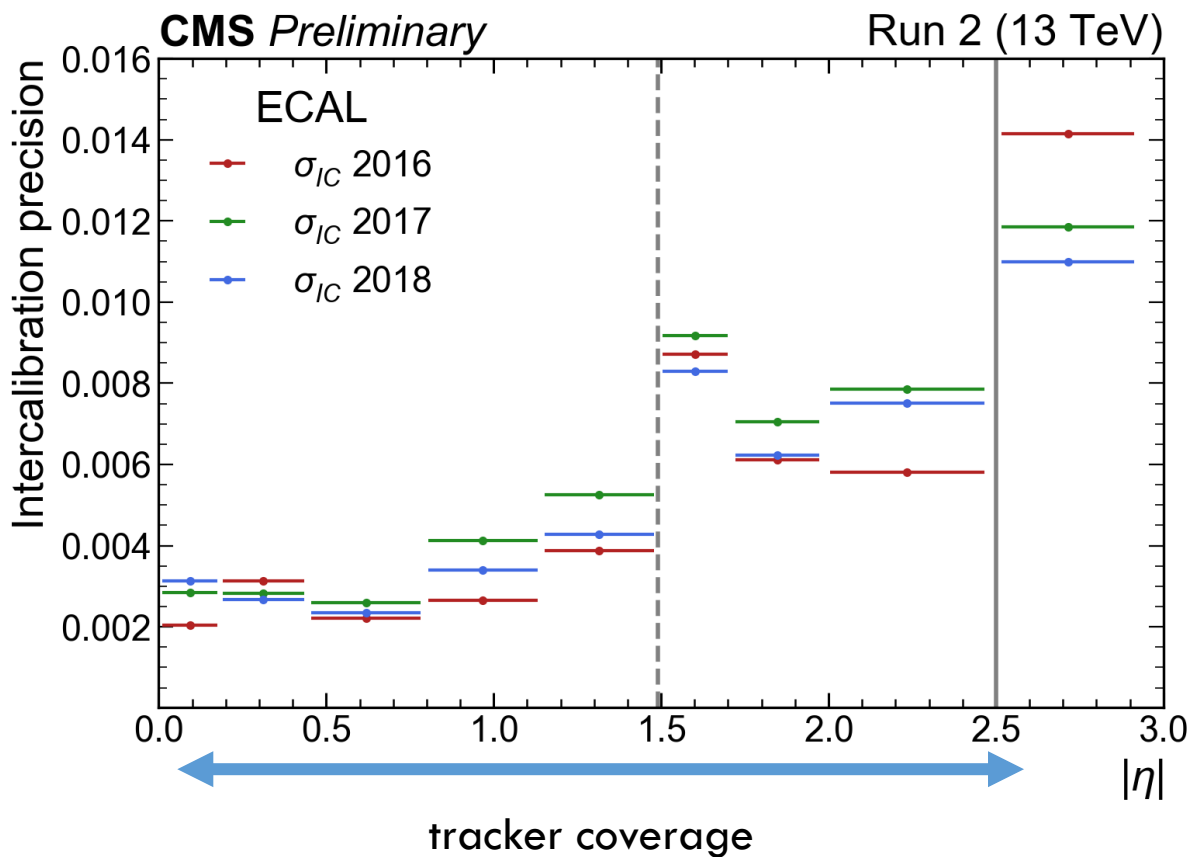
[CMS-DP2019-038](#)



Intercalibration precision

11

- Final intercalibration combines different methods by weighting their respective precision
 - precision evaluated with the relative energy resolution of Zee

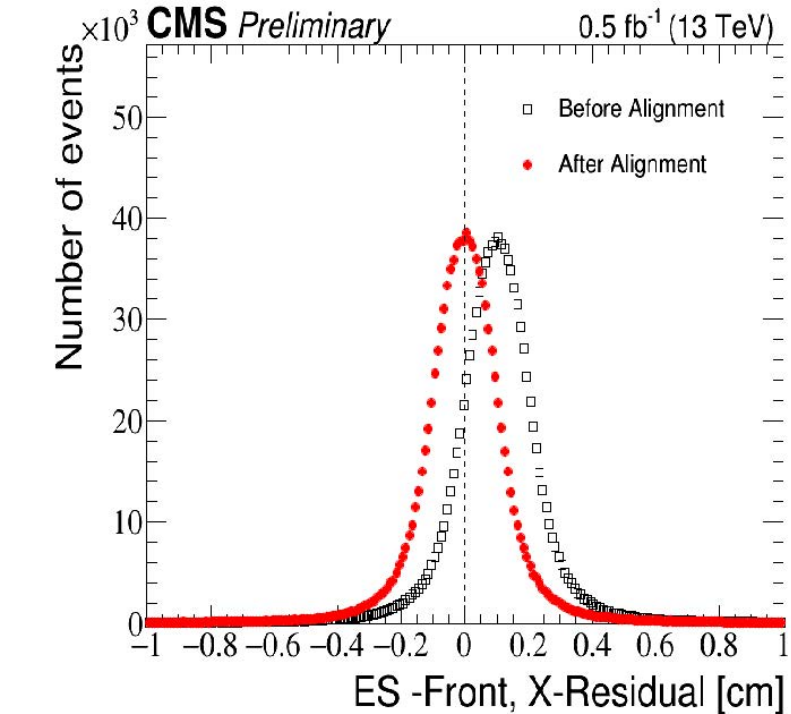
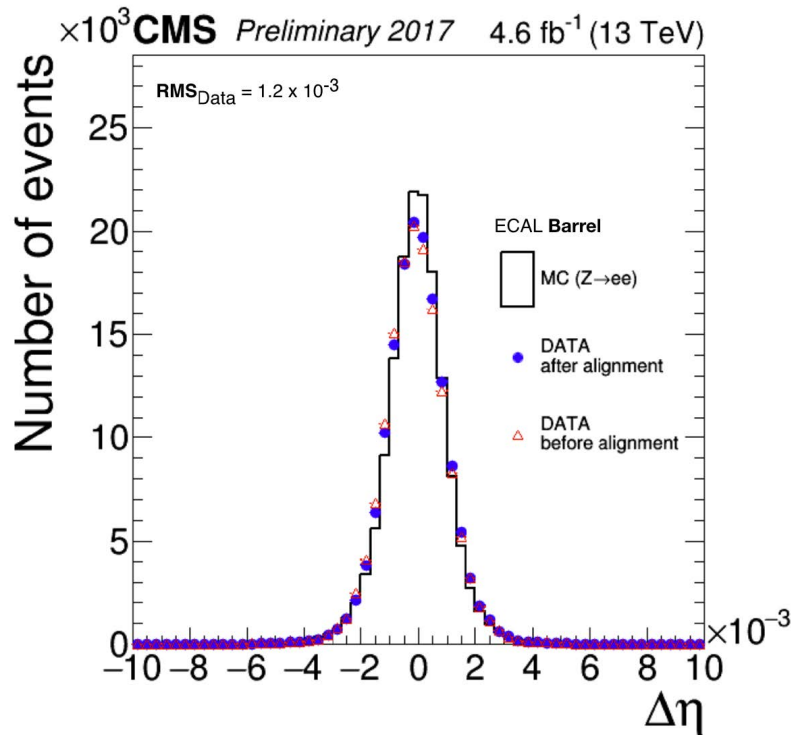


IC reaches very good precision

- $<0.5\%$ at barrel region
- $<1\%$ at endcap region

ECAL and Preshower (ES) alignment w.r.t the tracker in Run 2

12

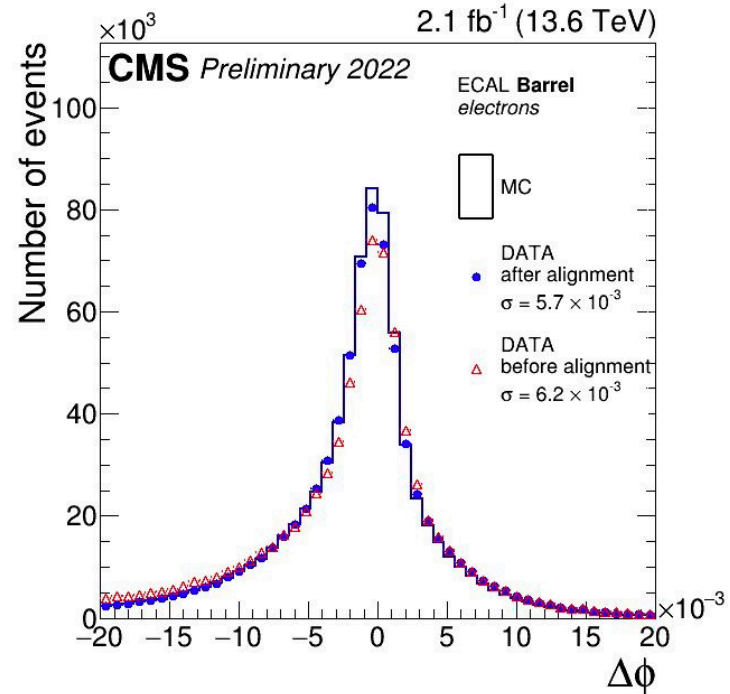
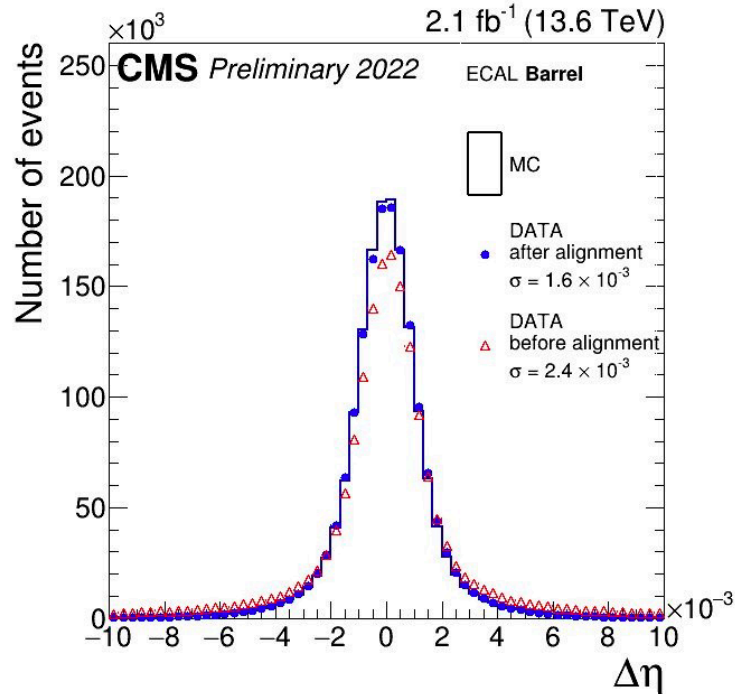


[CMS-DP2018-015](#)

- ECAL-tracker alignment: minimizing the difference in the η/ϕ between the ECAL super-cluster and the extrapolated track position
 - Using $Z \rightarrow e^+e^-$ events, check each e^+ and e^- , the distance between its track extrapolated from the tracker and its ECAL supercluster (SC) position
- ES-tracker: a minimization of the expected hit in the ES and the extrapolated track

ECAL alignment w.r.t. tracker in Run 3

13



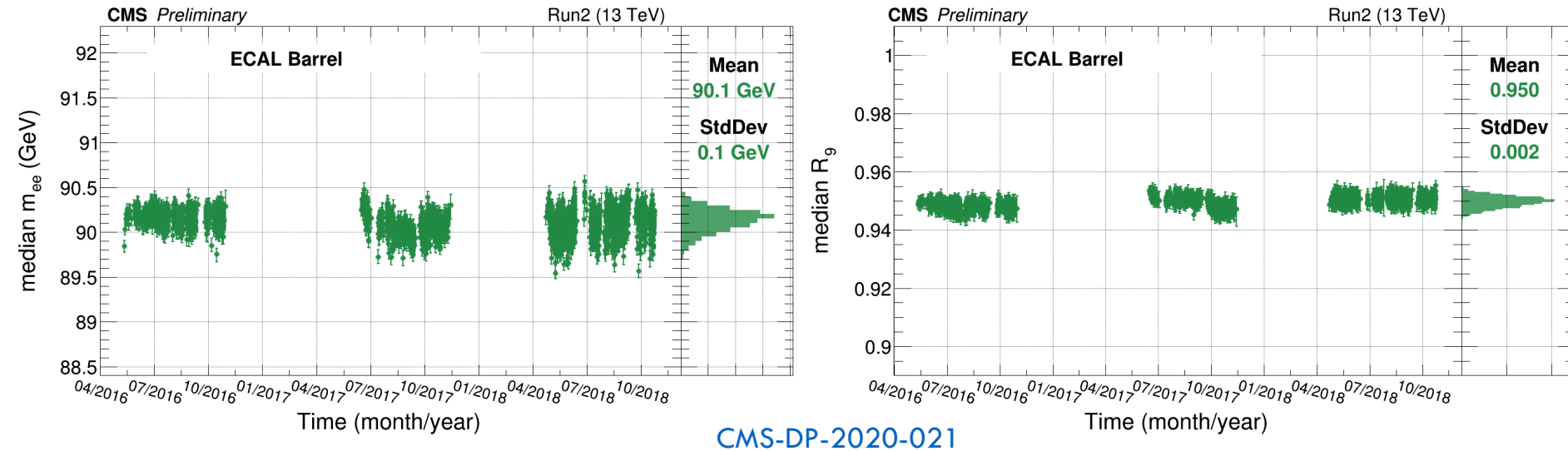
[CMS-DP2023-001](#)

- Relative alignment of ECAL crystals with the tracker detector using $Z \rightarrow e^+e^-$ events
- Prompt alignment calibration is important to data taken
 - E/Gamma trigger matching window needs to be loosen before the alignment, and tighten after alignment

ECAL performance in Run 2

14

- ECAL response is stable over time after corrections
 - validated with $Z \rightarrow ee$ events

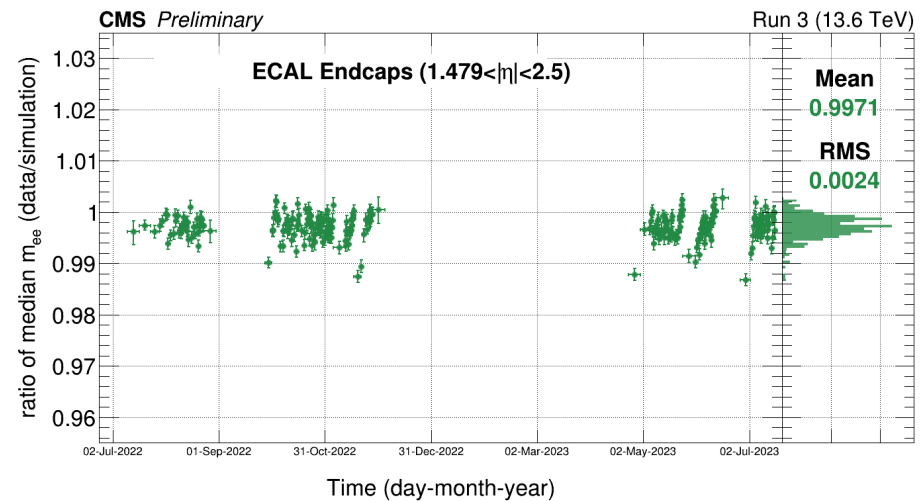
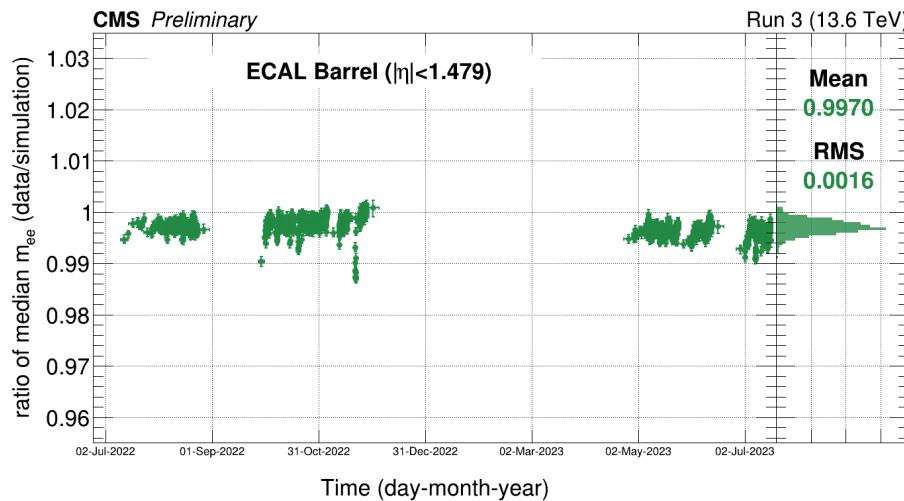


- energy scale stable at $\sim 1\%$ level across 3 years
- shower shape variable (R_9) also stable over time with spread $\ll 1\%$
 - R_9 : ratio of the energy deposit in the 3x3 crystal matrix around the seed crystal to that in the supercluster
 - important variable for the electron and photon identification

ECAL stability in Run3

15

The spread of the median ratio is at per mil level throughout 2022 and 2023.



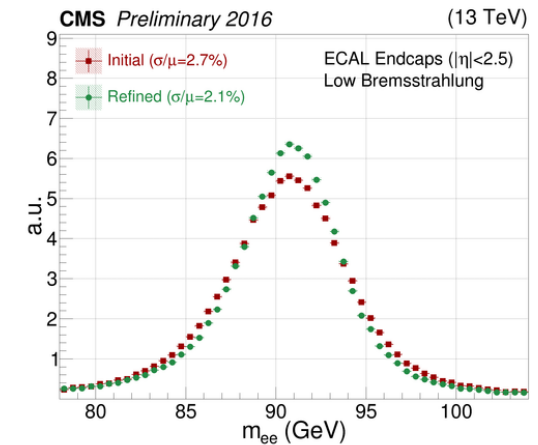
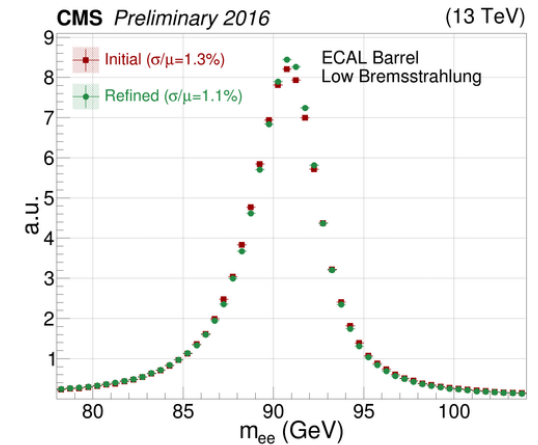
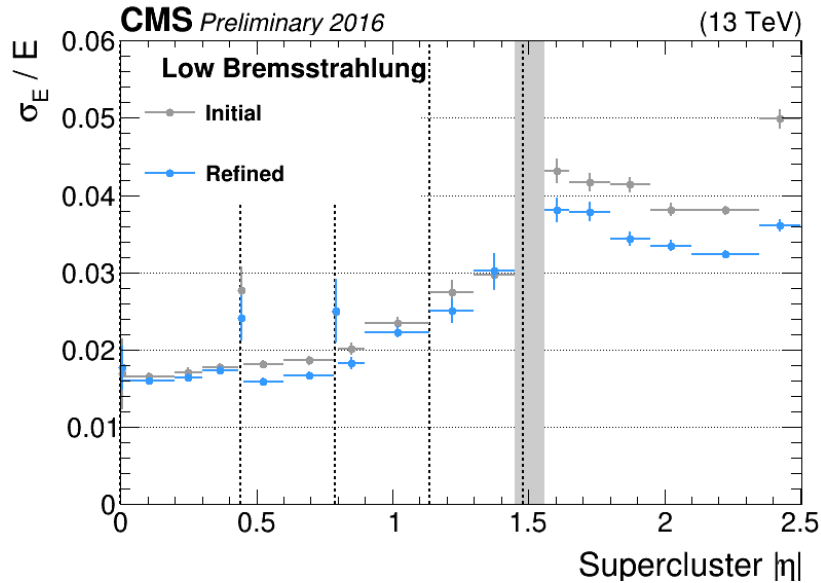
The median in data is slightly lower than in simulation due to resolution difference of the di-electron invariant mass distribution between the data and simulation, where the data shows a bit higher tail on the left caused by the time dependent effects that are difficult to be modelled in the simulation.

ECAL performance with calibration updates

16

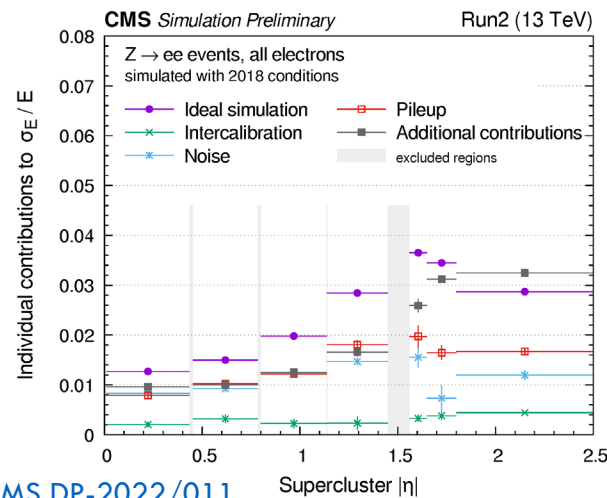
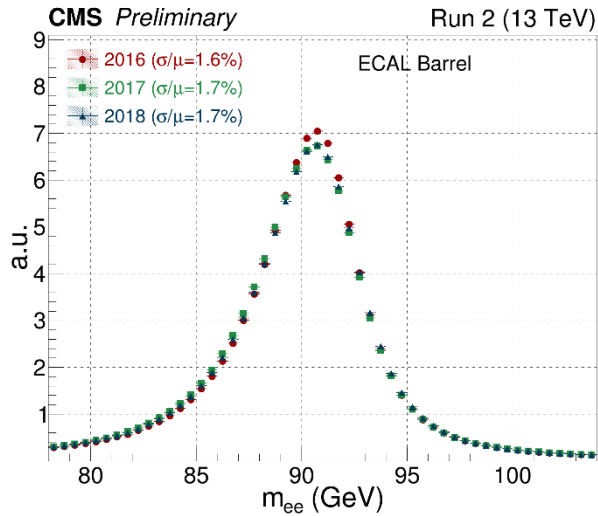
Two calibration sets for the full 2016 dataset: the "initial" calibration performed in 2017 and a "refined" re-calibration performed in 2019.

Di-electron invariant mass distribution for Z decay events
Relative electron (ECAL) energy resolution



ECAL performance in Run 2

17

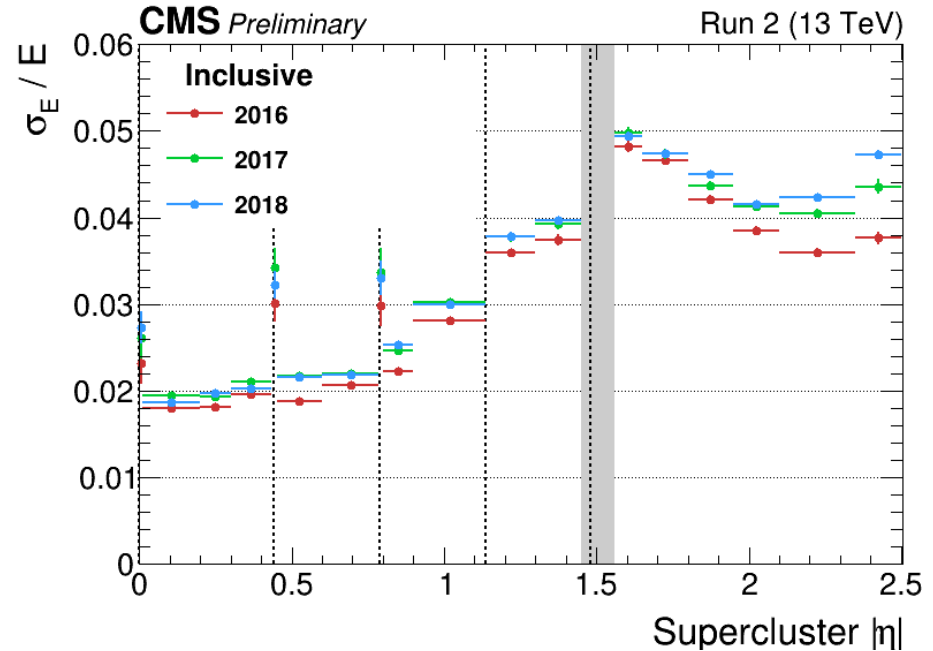


[CMS DP-2022/011](#)

Large impacts on resolution from pile-up and noise related effects

Energy and mass resolution with ECAL calibration

[CMS-DP-2020-021](#)



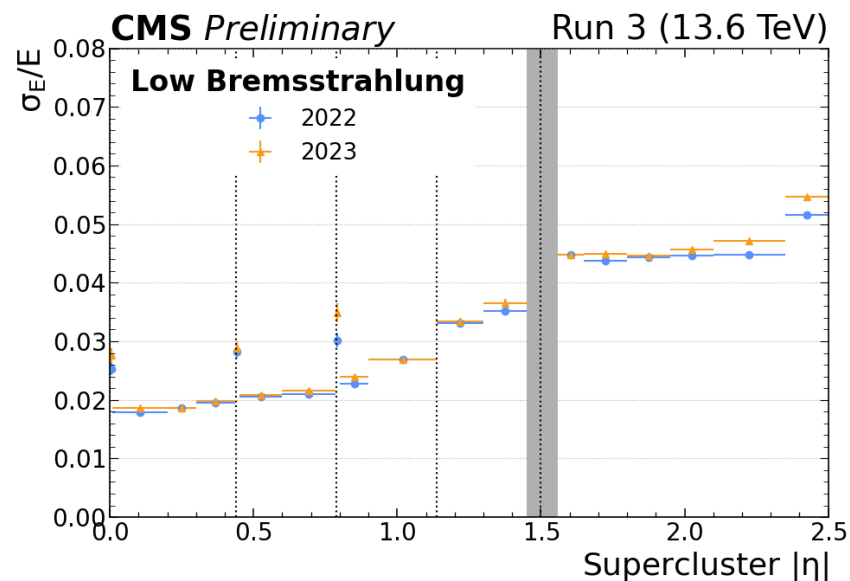
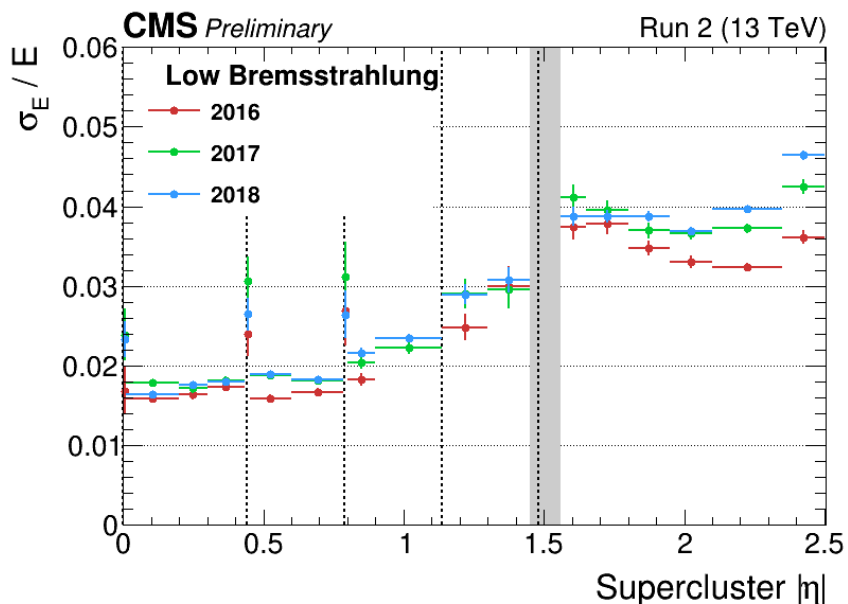
Excellent ECAL performance throughout Run 2

- resolution at $\sim 2\%$ in the central, $< 5\%$ elsewhere
- stable in different years in Run 2

ECAL performance Run2 and Run3

18

ECAL resolution degrades with detector aging over time, specially in the high eta range



Summary

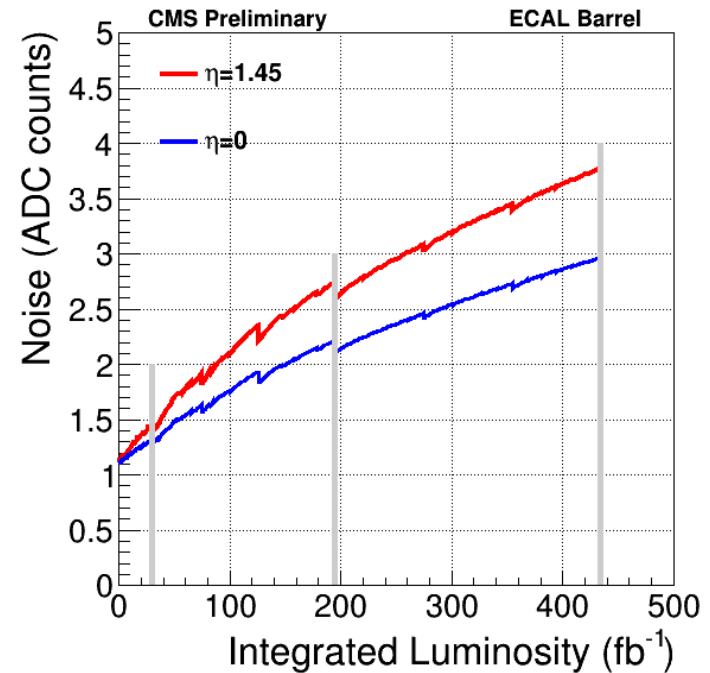
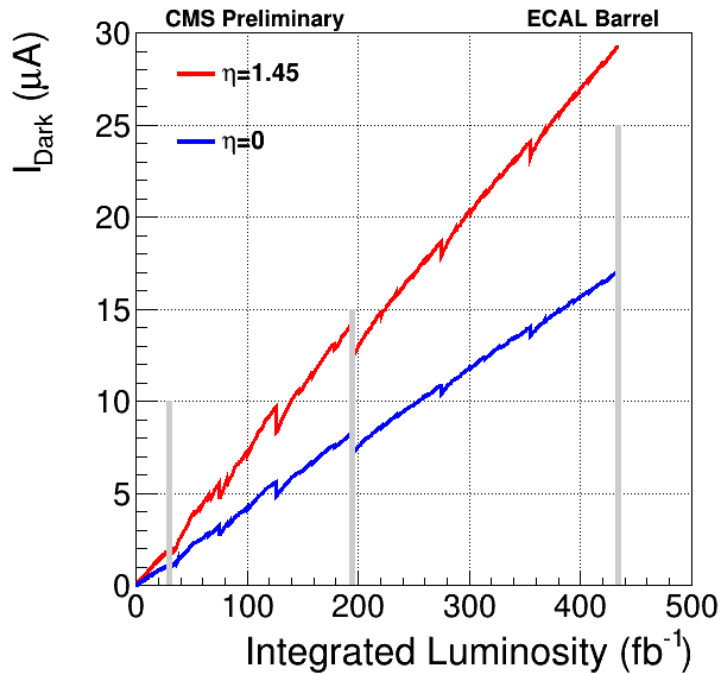
19

- Calibration and optimization has been exploited in CMS ECAL
 - challenging due to increased instantaneous luminosity and detector aging
 - new multifit method for amplitude reconstruction
 - frequent laser correction to stable ECAL response over time
 - combined intercalibration to stable crystal response at same η
- **Outstanding performance of the CMS ECAL with calibration**
 - stable ECAL response over time with spread at $\sim 1\%$ level
 - resolution of electrons **between 2% and 5%**
 - ECAL performance stable over time despite much harsher environment and detector aging
- ECAL group is constantly working to improve ECAL performance towards Run 3
 - more frequent laser condition updates, automation framework for prompt calibration, machine learning in clustering and monitoring etc..

Back Up

Evolving noise in ECAL

21



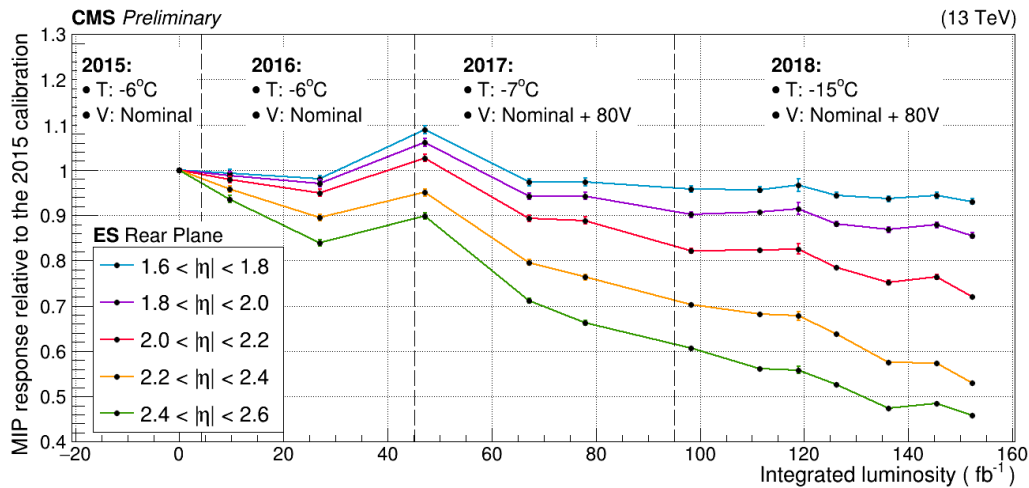
- ⊙ The leakage current in the ECAL Barrel APDs increases due to radiation-induced hadron fluence.
- ⊙ The noise increases due to the increase of the APD leakage current.

Preshower (E_{ES}) Calibration

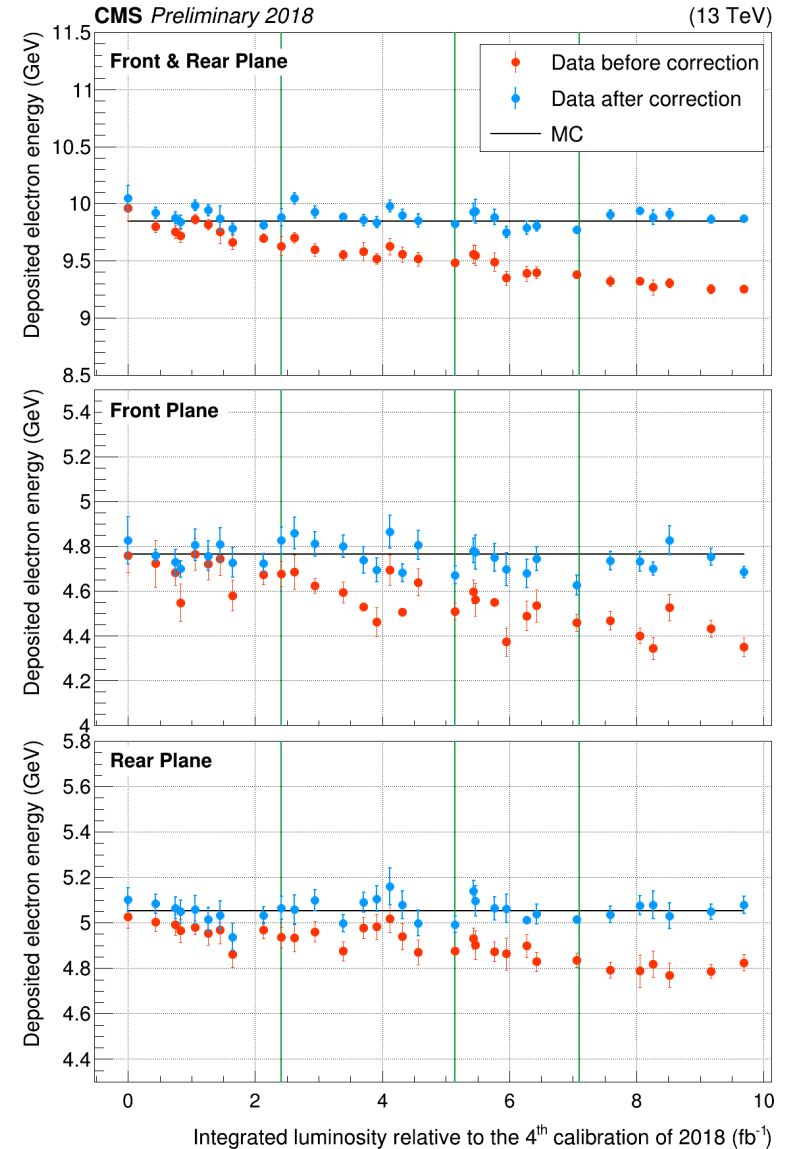
22

- Preshower calibrated using minimum ionizing particles (MIPs)
 - channel by channel calibration
 - special runs taken for calibration every 10 fb^{-1}

[CMS-DP-2019-038](#)



- correction computed by minimizing the χ^2 value between the energy distribution of data and MC using $Z \rightarrow ee$ events
- Measured energy of ES cluster is stabilized by applying the correction.

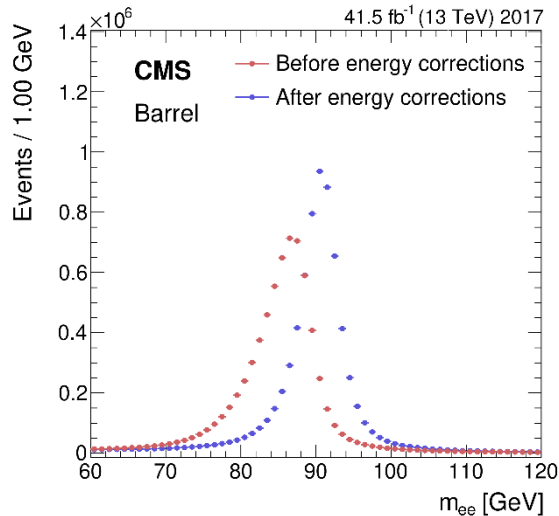
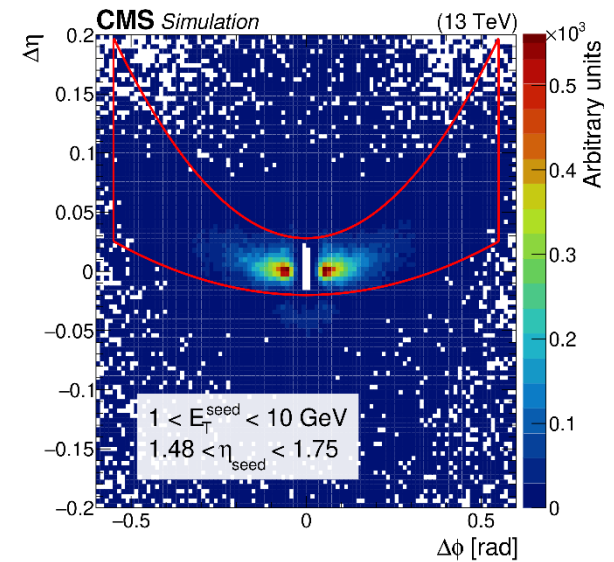


Clustering and cluster energy corrections ($F_{e,\gamma}$)

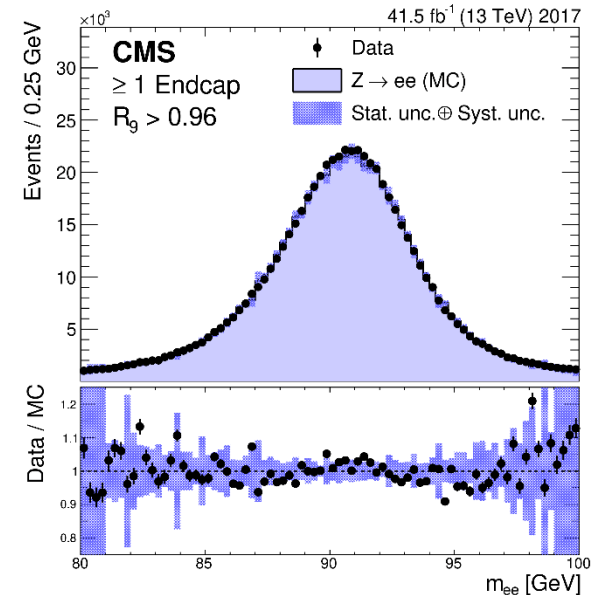
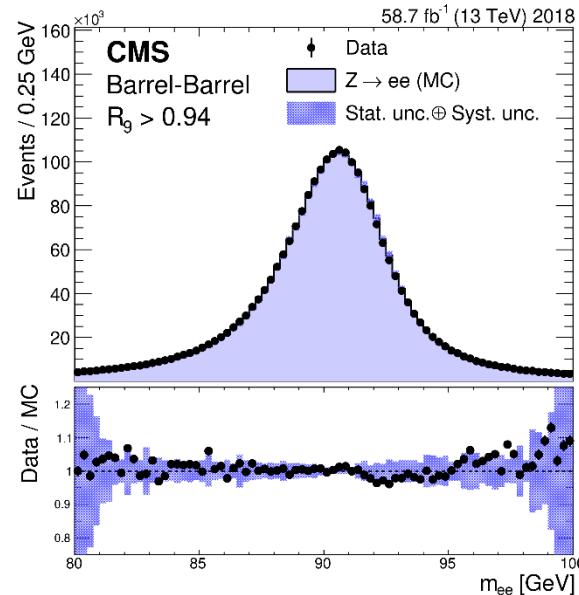
23

- ‘mustache super-clustering’ method exploits to cluster hits and form physics objects
- multivariate corrections applied to reconstruct the original deposited energy
- Energy thresholds for hits clustering re-tuned to mitigate pile-up and noise contamination
- Energy scale uncertainty smaller than 0.1 (0.3)% in the barrel (endcap) region in proton-proton collisions

[JINST 16 \(2021\) P05014](#)



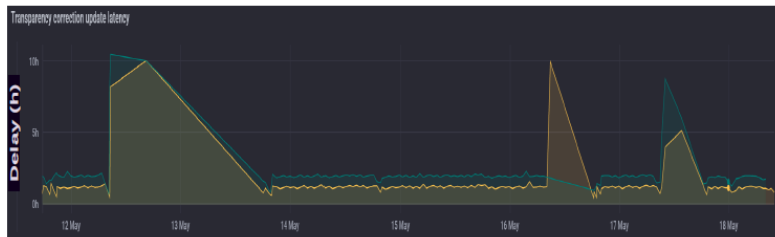
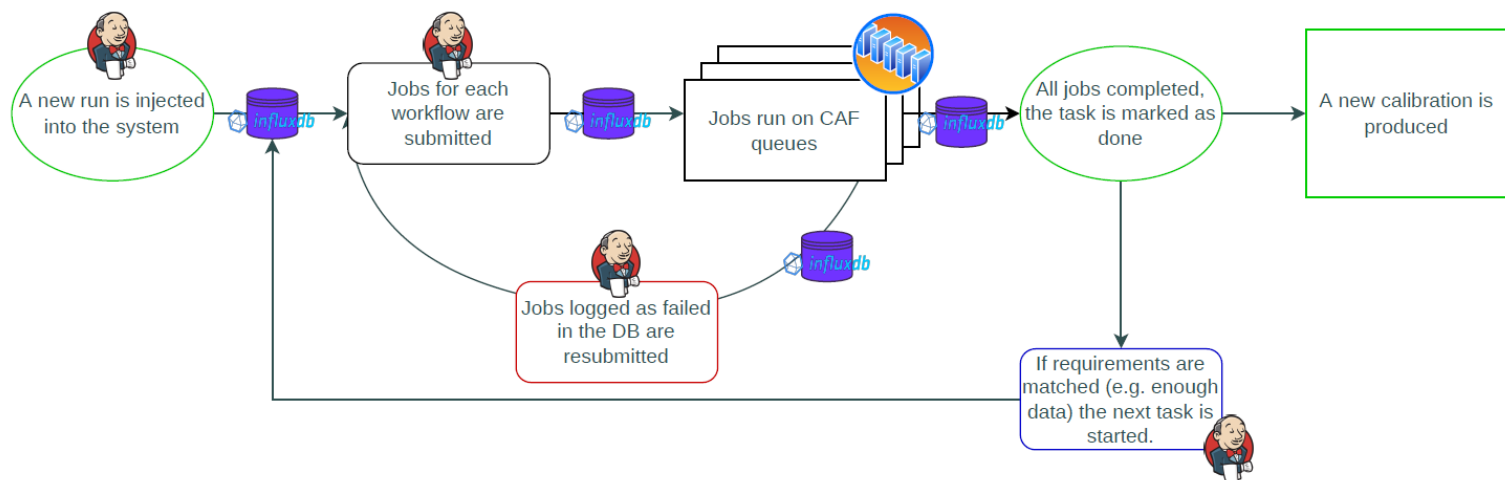
IHEP



Calibration of prompt reconstruction in Run3

24

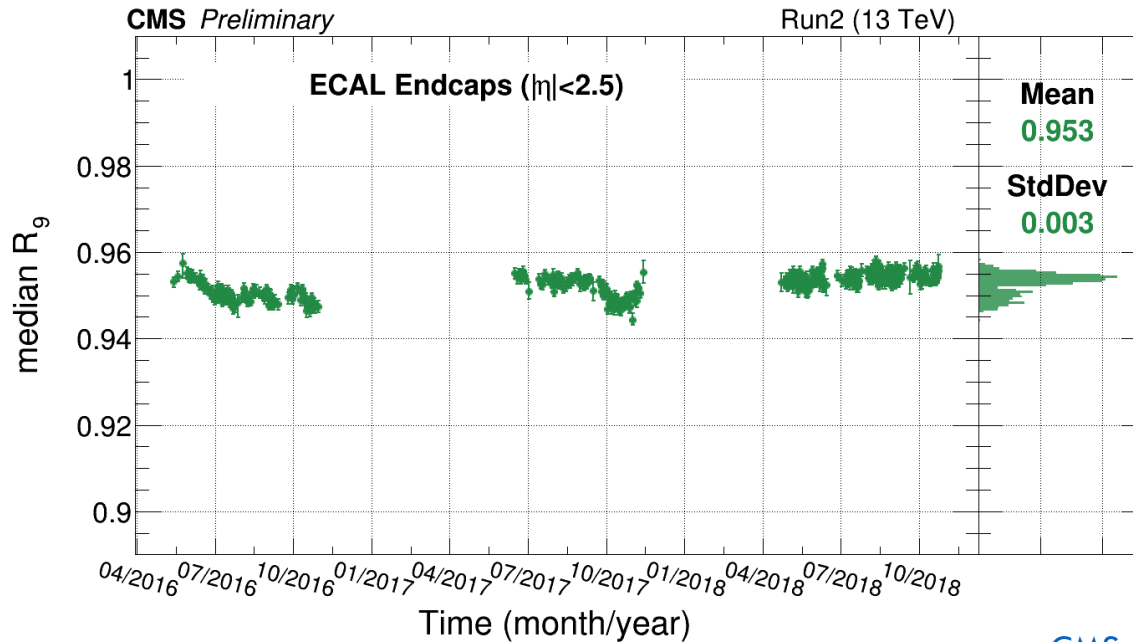
- Implement each calibration workflow as a finite state machine
- Execute jobs regularly updating conditions with predefined conditions
- Constant monitoring and update calibration with fine time granularity



System successfully
deployed in Run 3

ECAL time stability in endcaps

25

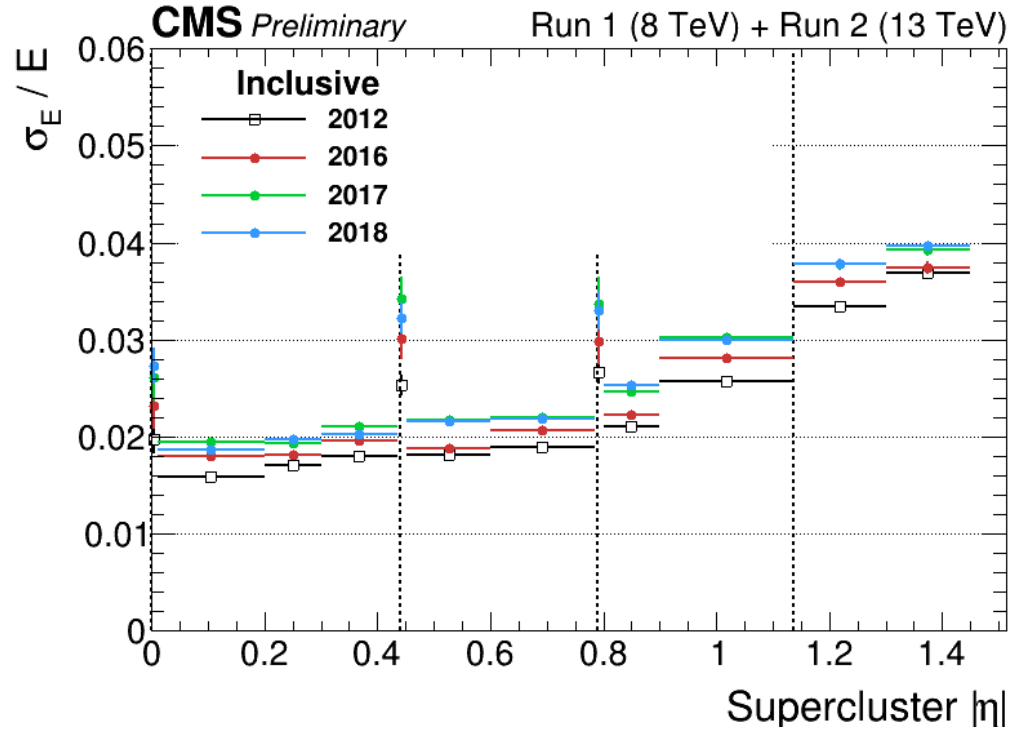


[CMS-DP-2020-021](#)

The shower shape is measured by the variable R_9 , defined as the ratio of the energy deposit in the 3x3 crystal matrix around the seed crystal to that in the supercluster. R_9 is responsive to changes in pedestal and noise.

ECAL performance in Run 2

26



- Similar performance in Run 2 and Run 1

Di-electron mass stability

Time stability of the di-electron invariant mass comparing between data and simulation for the 2022 and 2023 data-taking period using $Z \rightarrow ee$.

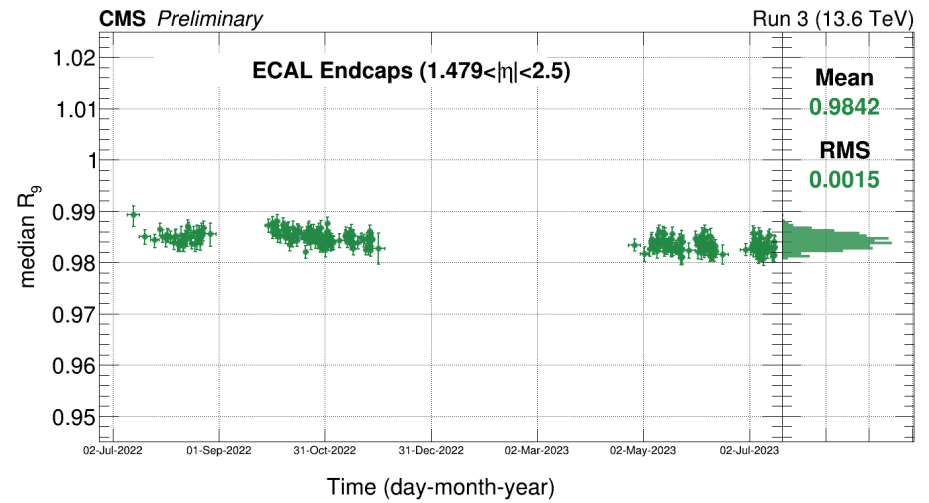
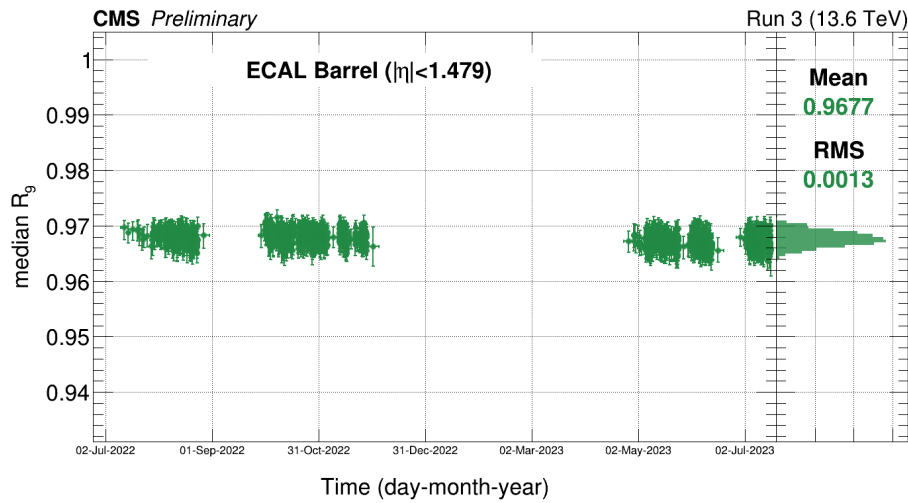
The plot shows the time stability of the di-electron invariant mass median ratio of data and simulation for the 2022 and 2023 dataset. Both electrons are required to be in the ECAL Barrel or in the ECAL Endcaps. The di-electron invariant mass is required to be between 70 GeV and 110 GeV. Each time bin has around 10000 events. The error bar on the points denotes the statistical uncertainty (at 95% confidence level) on the median. The right panel shows the distribution of the median ratios.

The median in data is slightly lower than in simulation due to resolution difference of the di-electron invariant mass distribution between the data and simulation, where the data shows a bit higher tail on the left caused by the time dependent effects that are difficult to be modelled in the simulation. The spread of the median ratio is at per mil level throughout 2022 and 2023.

Due to the recovery of the crystals during times without collisions, the pulse shape templates used for the amplitude reconstruction are updated from data after such periods as soon as enough data are available. For low statistic runs after a stop and before the update, the measured di-electron mass can show a lower value than for the rest of the time.

R9 stability

28



R9 stability

29

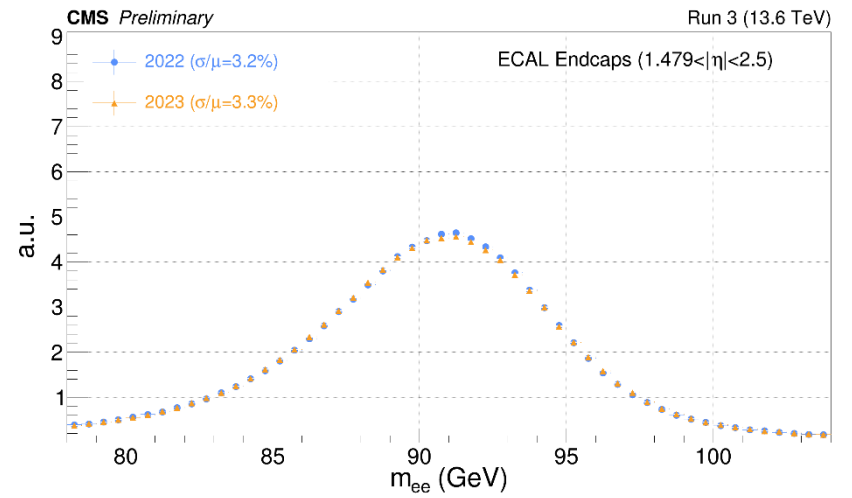
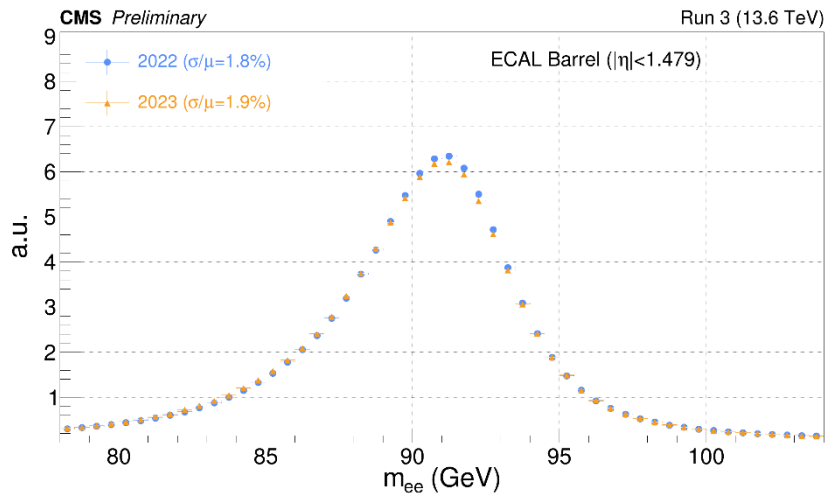
Stability of the shower shape of the electromagnetic deposit in the ECAL for the leading electron from Z decays.

The plot shows the time stability of the shower shape of the leading electron in Z decays with a refined re-calibration for 2022 and 2023 dataset. The event selection requires two electrons to be in the ECAL Barrel or in the ECAL Endcaps. The di-electron invariant mass is required to be between 70 GeV and 110 GeV. Each time bin has around 10000 events. The error bar on the points denotes the statistical uncertainty (at 95% confidence level) on the median. The right panel shows the distribution of the medians. The shower shape is measured by the variable R_9 , defined as in [EGM-18-002](#), the ratio of the energy deposit in the 3x3 crystal matrix around the seed crystal to that in the supercluster.

The shower shapes of the electromagnetic deposit in the ECAL are very stable in both 2022 and 2023.

Di-electron mass inclusive

30



Di-electron mass inclusive

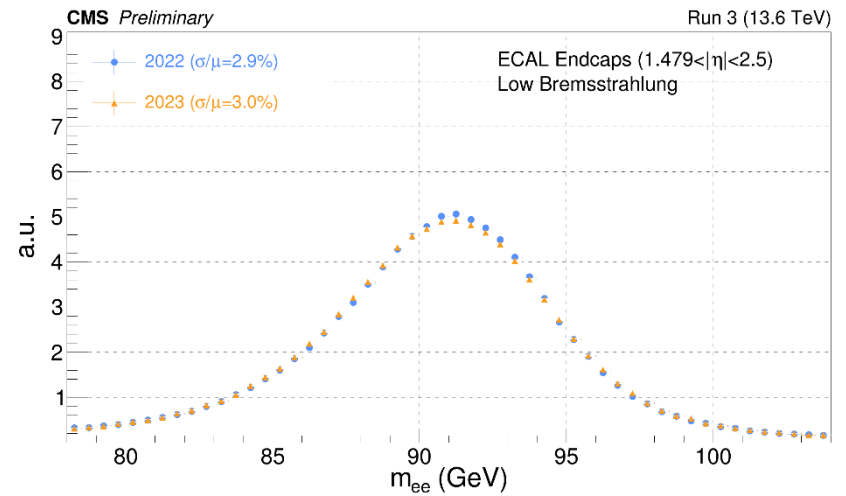
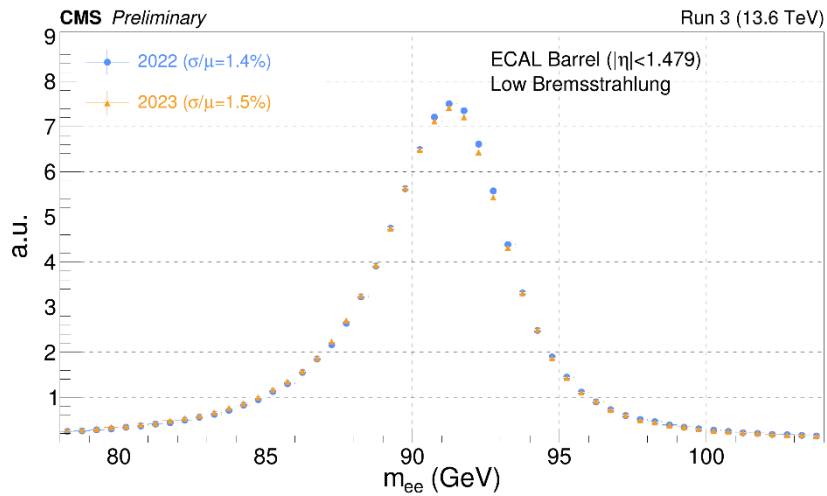
Invariant mass distribution for electron pairs from Z boson decays.

The plot shows the invariant mass distribution comparing 2022 and 2023 data-taking period using $Z \rightarrow ee$ events with a refined re-calibration. The event selection requires two electrons to be in the ECAL Barrel or in the ECAL Endcaps. For candidates in the Endcaps, the electron pseudorapidity is required to be lower than 2.5.

The inclusive resolutions of electrons are less than 2% in the barrel for both 2022 and 2023, and around 3.3% in the endcap in 2022 and 2023.

Di-electron mass low bremsstrahlung

32



Di-electron mass low bremsstrahlung

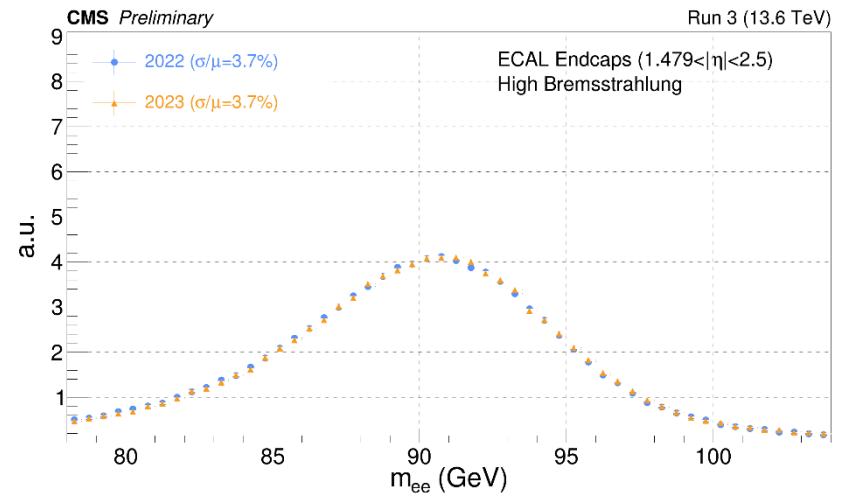
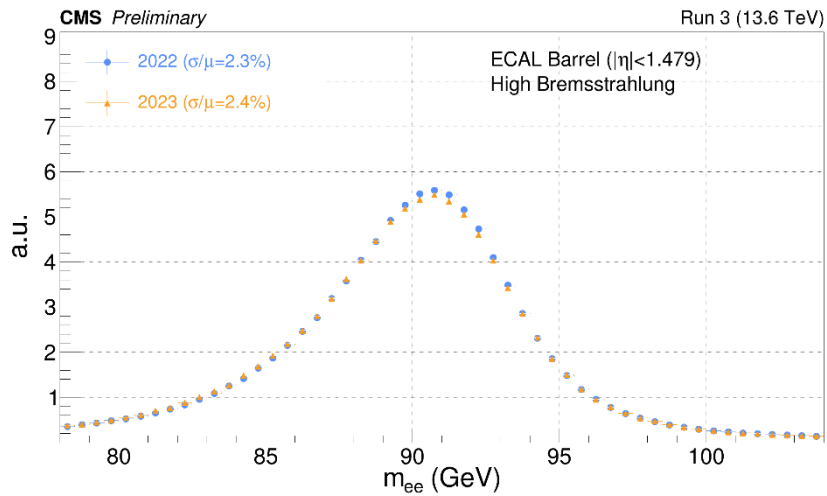
Invariant mass distribution for electron pairs from Z boson decays using low-bremsstrahlung electrons.

The plot shows the invariant mass distribution comparing 2022 and 2023 data-taking period using $Z \rightarrow ee$ events with a refined re-calibration. The event selection requires two electrons to be in the ECAL Barrel or in the ECAL Endcaps. For candidates in the Endcaps, the electron pseudorapidity is required to be lower than 2.5. For low-bremsstrahlung electrons, the shower shape variable of R_9 , defined as in [EGM-18-002](#), is required to be greater than 0.965.

The resolutions of low-bremsstrahlung electrons are around 1.5% in the barrel for both 2022 and 2023, and around 3% in the endcap in 2022 and 2023.

Di-electron mass high bremsstrahlung

34



Di-electron mass high bremsstrahlung

35

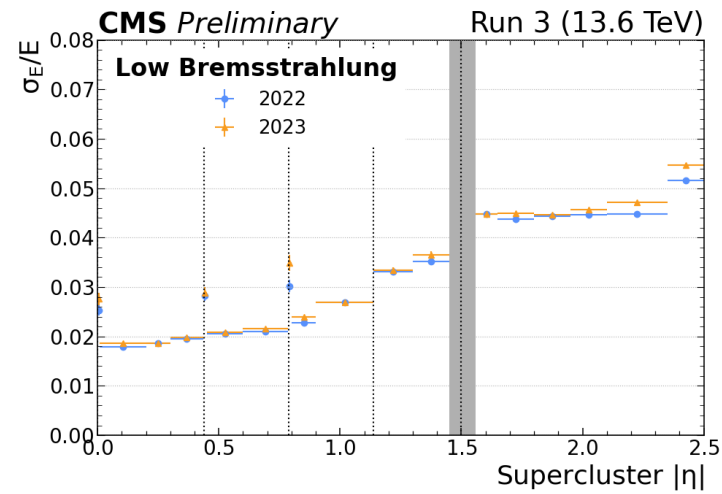
Invariant mass distribution for electron pairs from Z boson decays using high-bremsstrahlung electrons.

The plot shows the invariant mass distribution comparing 2022 and 2023 data-taking period using $Z \rightarrow ee$ events with a refined re-calibration. The event selection requires two electrons to be in the ECAL Barrel or in the ECAL Endcaps. For candidates in the Endcaps, the electron pseudorapidity is required to be lower than 2.5. For high-bremsstrahlung electrons, the shower shape variable of R_9 , defined as in [EGM-18-002](#), is required to be less than 0.965.

The resolutions of high-bremsstrahlung electrons are around 2.4% in the barrel for both 2022 and 2023, and around 3.7% in the endcap in 2022 and 2023.

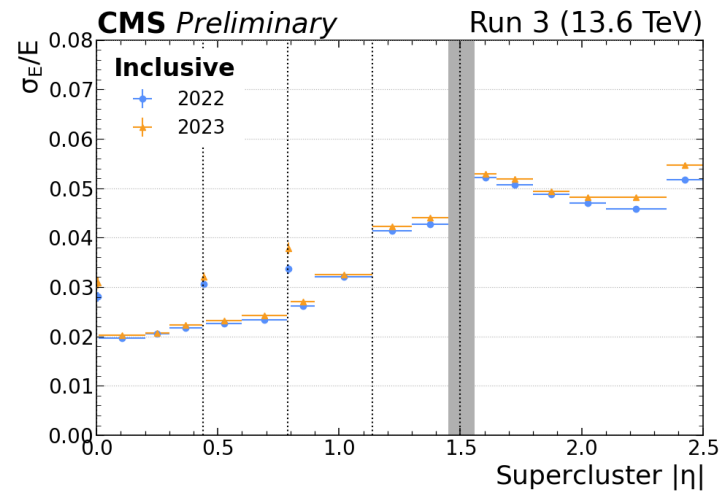
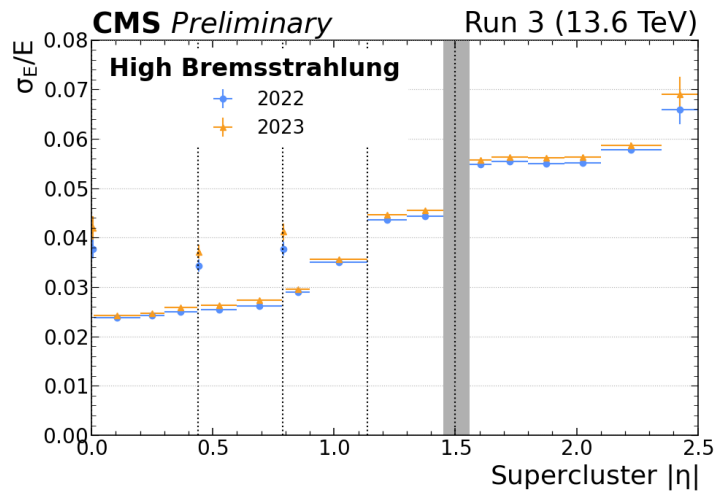
ECAL Resolution – low bremsstrahlung

36



ECAL Resolution – inclusive, high bremsstrahlung

37



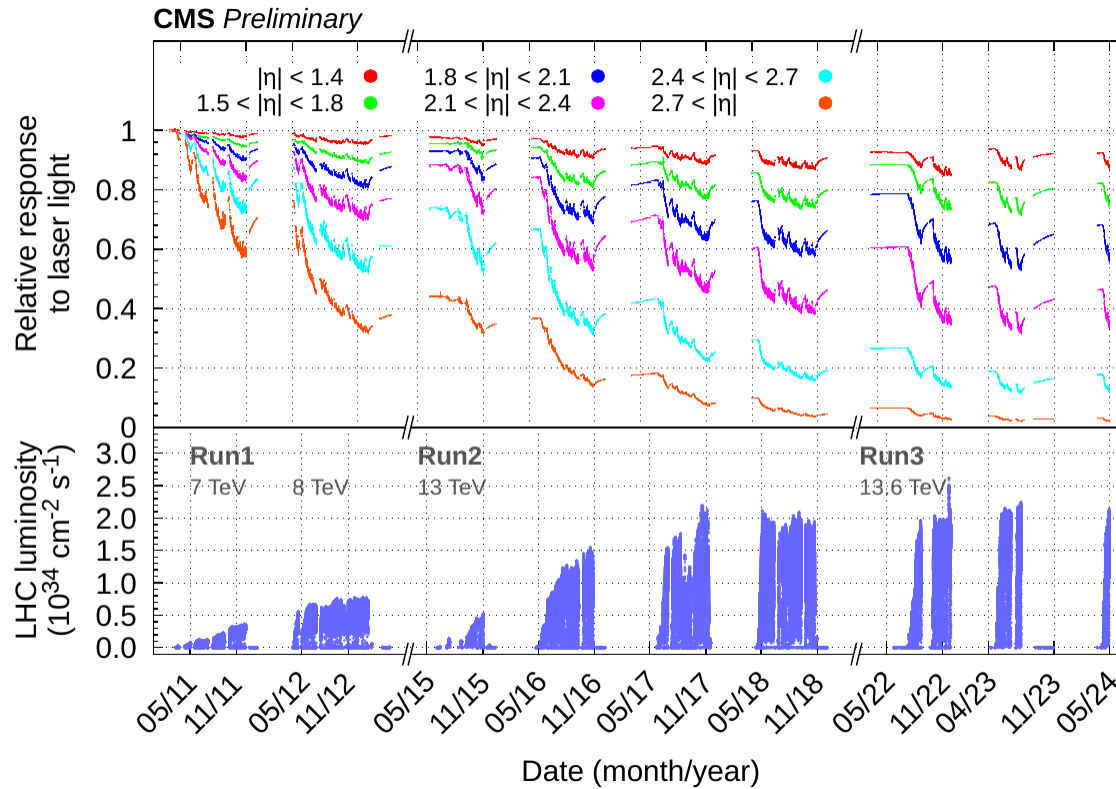
ECAL Resolution

Relative electron (ECAL) energy resolution unfolded in bins of pseudorapidity η . Electrons from $Z \rightarrow ee$ decays are used. The resolution is shown separately for low-bremsstrahlung electrons, high-bremsstrahlung and for all electrons ("inclusive"). The plot compares the resolution achieved after a refined calibration of the data collected during 2022 and 2023 at 13.6 TeV. The relative resolution σ_E/E is extracted from an unbinned likelihood fit to $Z \rightarrow ee$ events, using a Voigtian (Breit-Wigner convolved with Gaussian) as the signal model. The vertical bars on the points represent the statistical uncertainty. The vertical dotted lines mark the boundaries between the ECAL modules in the barrel, where a slight worsening of the resolution is observed due to the material of the mechanical structures. The shaded grey band corresponds to the Ecal Barrel/Ecal Endcap (EB/EE) transition.

A stable ECAL energy resolution is observed between 2022 and 2023 despite the increased LHC luminosity and the ageing of the detector.

Laser history plot

39



Laser history plot

Relative response to laser light (440 nm in 2011 and 447 nm from 2012 onwards) injected in the ECAL crystals, measured by the ECAL laser monitoring system, averaged over all crystals in bins of pseudorapidity (η), for the 2011, 2012, 2015, 2016, 2017, 2018, 2022, 2023, and part of 2024 data taking periods, with magnetic field at 3.8 T. The response change observed in the ECAL channels is up to 15% in the barrel and it reaches up to 70% at $|\eta| \approx 2.5$, the limit of the tracker acceptance. The response change is up to 99% in the region closest to the beam pipe. The recovery of the crystal response during the periods without collisions is visible. The relative response to laser light for $|\eta| < 1.4$ at the beginning of 2023 is higher than in 2022 due to an update of the high voltage settings applied to compensate for the APD gain change. These measurements, performed every 40 minutes, are used to correct the physics data. This is an update of the plots appearing in CMS-DP-2012/007, CMS-DP-2012/015, CMS-DP-2015/016, CMS-DP-2015/063, CMS-DP-2016/031, CMS-DP-2017/003, CMS-DP-2017/023, CMS-DP-2018/015, and CMS-DP-2022/042 and includes measurements taken up to May 2024. The bottom plot shows the instantaneous LHC luminosity delivered during this time period. The instantaneous luminosity is calculated for a clearly defined short data segment called a lumi section, which is set to about 23s.

The 2023 laser response starts with a higher value than the 2022 response in EB, caused by the change of the HV gain in EB at the beginning of 2023 which changed the laser response and was absorbed in the ICs. See https://indico.cern.ch/event/1268299/contributions/5327279/attachments/2615972/4521384/GainChange_2023.pdf